Dynamic Hierarchical Self-Assemble Small Molecule Structure Hexabenzocoronene for the High-Performance Anodes Lithium Ion Storage

Dawei He[1], Fuyan Xiao[3], Zhou Wang[2], Aolin He[1], Ruijiang Liu[3] and Guofan Jin[3*]

Abstract

This study examined the characteristics of small molecular structure nano-graphene in a dynamic hierarchical self-assembly and found that graphene is rearranged under its own pressure during dynamic aggregation and water ripples are formed by the *d*-spacing. The composition and structure were studied using a range of material characterization techniques. No covalent bonds were observed between molecules, and the self-assembled driving force was the only intermolecular interaction: Van der Waals' force in the intra-layer and π–π interactions between layers. The arranged-rearranged structures provided a range of lithium ion shuttle channels, including the space between layers and diffusing through the nanosheets, which decrease the diffusion distance of lithium ions remarkably and reduce the irreversible capacity of the battery.

Keywords: Hexabenzocoronene, Dynamic hierarchical self-assemble, *d*-spacing, Rearrange

Introduction

The development of green alternative energy sources has received considerable interest. Recently, nano-graphene and graphene composites attracted interest for used as lithium ion anodes [1–3]. In addition, a variety of core–shell structures with carbonaceous materials encapsulated silicon or metal nanostructure have been proposed to alter the performance of the anode materials [4]. Furthermore, graphene is one of the most promising materials to replace graphite and has been studied widely since Professor Andre Konstantin Geim and Konstantin Sergeevich produced stable graphene in 2004 using the deceptively simple Scotch tape method [5, 6]. Other methods of producing graphene include liquid phase and thermal exfoliation [7–9], chemical vapor deposition [10, 11], and synthesis on SiC [12, 13]. Graphene has a hexagonal honeycomb lattice structure, and its amazing properties have stimulated strong interest [14–20].

Hexabenzocoronene (HBC, hereafter) is a representative example of nano-graphene that has been well studied [21–30]. The smaller modular sizes and size-tunable are the main features. HBC is one of the allotropes of carbon with a layered structure of sp^2 carbon atoms. Each layer has a hexagonal honeycomb structure called a nano-graphene sheet (Fig. 1) [31]. While the chemistry of nano-graphene has been well established, its ability to overlap and aggregate in a generalized nano-morphology molecule is not completely understood. Therefore, determining how nano-sized graphene molecules are stacked and how the stacked sheets interact is important.

This paper introduces the dynamic hierarchical self-assembly structure–function relationship of hexabenzocoronene. By observing the *d*-spacing generated via the dynamic self-assembly at the molecular level and the relationship between the clusters of nano-graphene, an in-depth analysis of the formation factors inside of nano-graphene was analyzed further.

* Correspondence: organicboron@ujs.edu.cn
[3]School of Pharmacy, Jiangsu University, Zhenjiang 212013, People's Republic of China
Full list of author information is available at the end of the article

He *et al. Nanoscale Research Letters* (2019) 14:65

Page 2 of 8

Fig. 1 Hexabenzocoronene structure and self-assembly diagram
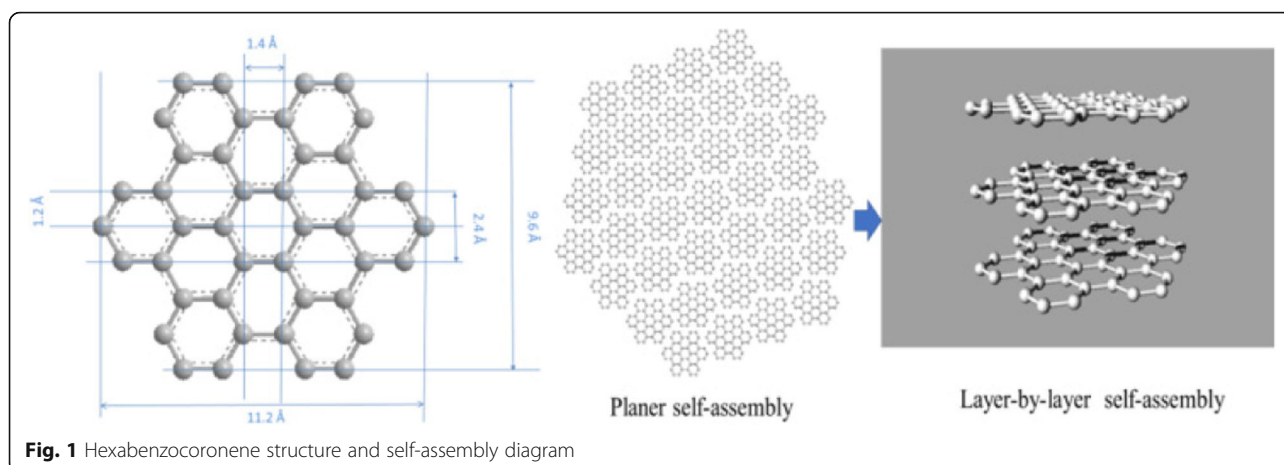
Methods/Experimental

Materials

Hexabenzocoronene was synthesized according to a previously reported procedure [32–35]. All solvents were freshly distilled from proper dehydrating agents under argon gas. All chemicals are analytical grade and purchased from Shanghai Chemical Corp. Thin-layer chromatography (TLC) was performed on silica gel 60 F254 (Merck DGaA, Germany). The electrolyte solution was purchased from Shanghai Annaiji Technology Co., Ltd. The electrolyte solution is made up from 0.1 M tetra-*n*-butylammonium perchlorate (TBAP). Deionized water is used for all experiments.

Characterization

The morphology and lattice fringe were observed using a scanning electron microscope (SEM, JEOL JCM-6000Plus), transmission electron microscope (TEM, JEOL H-7000), and high-resolution transmission electron microscope (HRTEM, JEOL JEM-2100).

Electrochemical Measurements

Electrochemical measurements were performed on the Shanghai Chenhua CHI660e system. A three-electrode system is used, a platinum wire for the counter electrode, a platinum plate with a fixed of electrode, and a saturated calomel electrode for the reference electrode. The concentration of the supporting electrolyte TBAP was 0.1 mol/L, and the analytical pure solvent was acetonitrile (ACN). Firstly, polish the platinum carbon compound electrode vertically on the circular gauze on the glass brick (paint "8", 0.05 μm aluminum powder and water as friction agent); secondly, rinse off the white aluminum with distiller water and then use ultrasonic for 1 min by acetone; and finally, use ear ball washed and blown dry. Then, the suspension of the hexabenzocoronene sample was dropped on the surface of the glassy carbon compound electrode, and the solvent was naturally evaporated to dryness. Then 0.1 M tetra-*n*-butylammonium perchlorate and 0.1 mM ferrocene electrolyte solution were scanned at a scan rate of 0.1 mV s^{-1}.

Results and Discussion

Hexabenzocoronene is carbon–carbon material combined with significant π–π conjugate chemical bonding. A procedure for the preparation for hexabenzocoronene consisted of a series of reactions, such as Sonogashira, Diels-Alder reaction, Lewis catalyst-based cycle reaction, and deprotonation under basic conditions to give intermediates in unsatisfactory yields [36–38]. The target compounds are generated from intermediates and nitromethane with the treatment of a Lewis reagent gave the target compounds in a similarly low yield [39, 40]. The reaction solution was quenched with methanol, followed by repetitive dissolution and precipitation with methylene chloride/methanol. The collected crude compounds were washed with methanol/acetone (1:1) to give a yellowish solid (see Additional file 1) [41, 42].

HBC has been widely used, but in the study of self-assembled system, it needs to be further understood. Although studies of the same or similar anode materials have been mentioned in the reported literature, the HBC study is still insufficient. Therefore, the focus of the work is on the detailed research of the self-assembly system, and put it on one by one to understand the internal dynamic distribution of aggregation and the induction and to improve the supplement of the lack of content anode materials.

The small-molecule nano-graphene self-assembled dynamically to form regular thin sheets, which were sequentially and systematically stacked to form intermittent sheet nano-graphene fragments that were held tightly to each other [43]. On the other hand, the dynamic self-assembled aggregate structure was superimposed on the subject to rearrange/change under

stress, thereby forming an uneven gear shape [44, 45]. Owing to the size of the nano-graphene itself, there was no obvious bulge in the overall structure. As shown in the figure, the entire nano-aggregation was regular, like a fingerprint shape (Fig. 2).

To explain the abovementioned rearrangement/change caused by its own weight and whether it will affect the material properties, scanning electron microscopy (SEM) was performed to determine if the particle size had changed. As shown in Fig. 3, the nanoparticles are gathered together and their particle size was unaffected by the rearrangement/change. The SEM image clearly shows that nano-graphene was distributed uniformly as nanoparticles. In addition, daisy-like clusters, 200, 50, and 20 nm in range, were observed. Their end parts were stretched outward with certain regularity, which is densely concentrated like a flower pattern. Therefore, the self-assembly process of nano-graphene sheets can be carried out in two ways. First, the nano-graphene molecules are self-assembled by overlapping the edges. Second, nano-graphene molecules overlap with each other, which enables the self-assembly of molecules.

Transmission electron microscopy (TEM) showed that the hexabenzocoronene molecule exhibits structural features with a coherent layer spacing and a molecular layer spacing from 0.34 nm. High-resolution TEM (HRTEM) indicated that nanoparticles bind to each other (Fig. 4) [46, 47]. The concentric diffraction rings in the selected area electron diffraction (SAED) pattern confirm the polycrystalline nature of hexabenzocoronene. Furthermore, the HRTEM image shows that most of the graphene-like walls consisted of a few layers (≈ 14 layers), indicating typically ultrathin structures [48–51]. The layer-by-layer structures of the hexabenzocoronene

and the perfect *d*-spacing between the layers highlight the performance of LIB anode materials.

The voltage profiles of hexabenzocoronene and the performance were measured using a cycling test. Figure 5 shows the capacity of the electrode at various current densities and the corresponding voltage profiles. The capacity at 100 cycles is 200 mAh/g, and good reversibility was observed with a coulombic efficiency over 98%.

Cycle voltage (CV) was performed at the high potential of the lithium-ion batteries to determine the long-term stability and potential energy (Fig. 6a). According to the above description, CV (Li$^+$/Li vs Ag/AgCl) was further undertaken to understand the lithium storage behavior. The CV curves hexabenzocoronene were measured at the same scan rates (0.1 mV s^{-1}) and display redox peaks with slight shifts with increasing scan rates, thereby showing a rectangular shape with increasing scan rates, as shown in Fig. 6. The twisted rectangular shape at a fast scan rate may be due to the poor electronic nature of the polycrystalline materials, as proposed by Dunn et al. The measured highest occupied molecular orbital (HOMO) energy at a fixed potential (V) can be separated into oxidation increases (V_1), standard oxidation effects (V_2), and standard reduction effects (V_3) (Eq. (1)), which can quantitatively characterize the capacity contribution of each part.

$$\mathrm{HOMO}(V) \;=\; V_1 \;-\; V_2 \;+\; V_3 \qquad (1)$$

The anion/radical anion with an electron donating functional group leads to a homogeneous/uniform electron distribution throughout the flake, which is beneficial for maximizing the number of Li$^+$ incorporated into
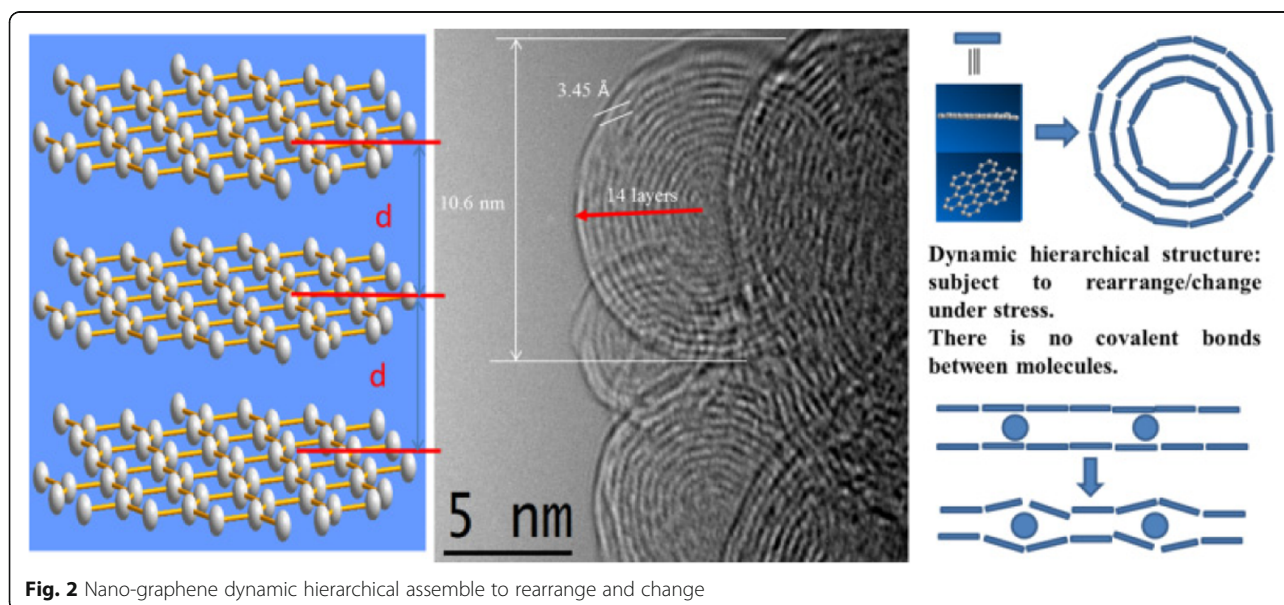
Fig. 2 Nano-graphene dynamic hierarchical assemble to rearrange and change

Fig. 3 SEM and TEM images for hexabenzocoronene

Fig. 4 HRTEM image of hexabenzocoronene with their dynamic hierarchical assembles
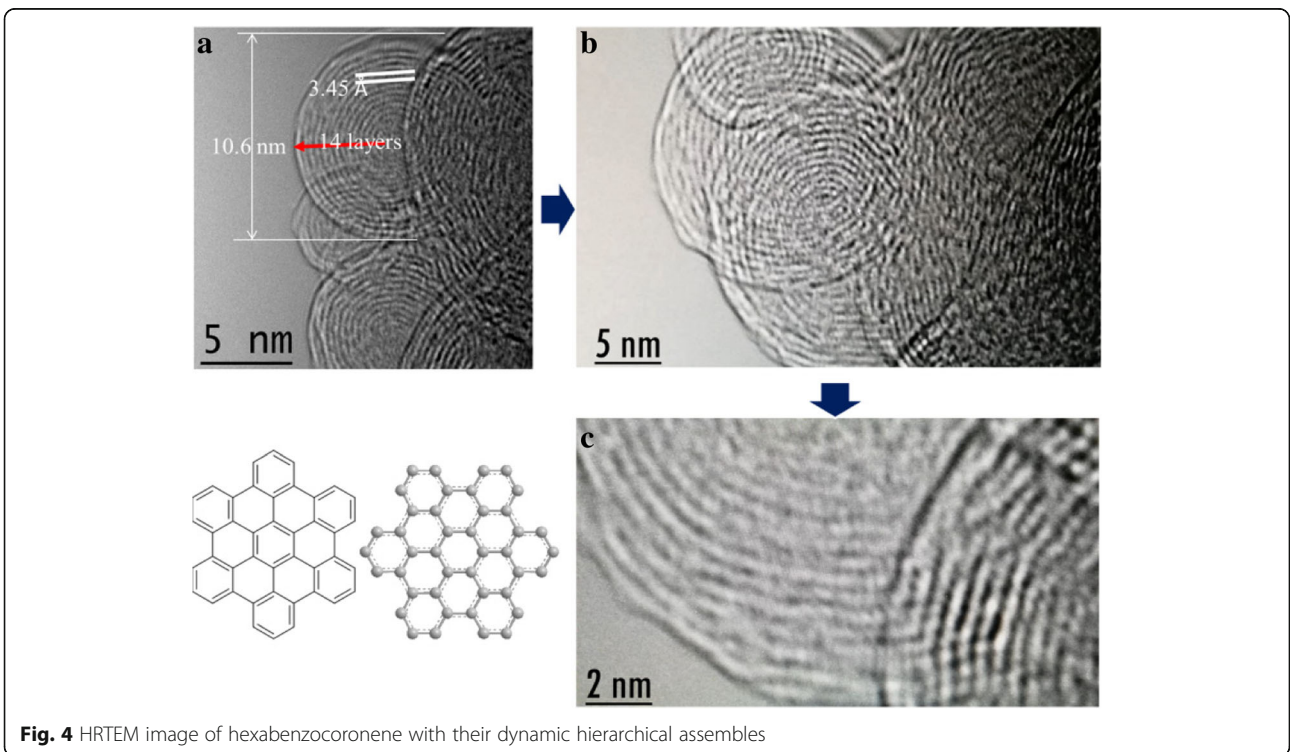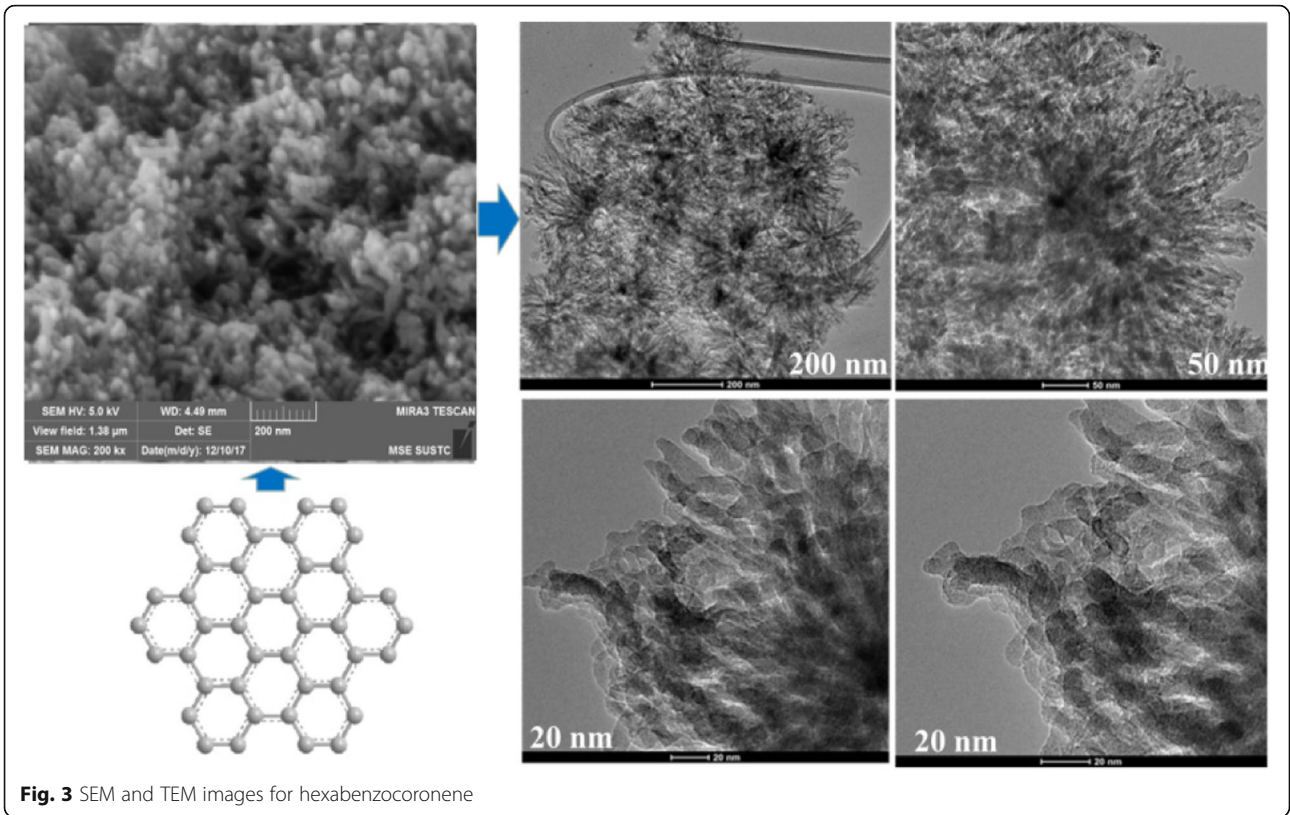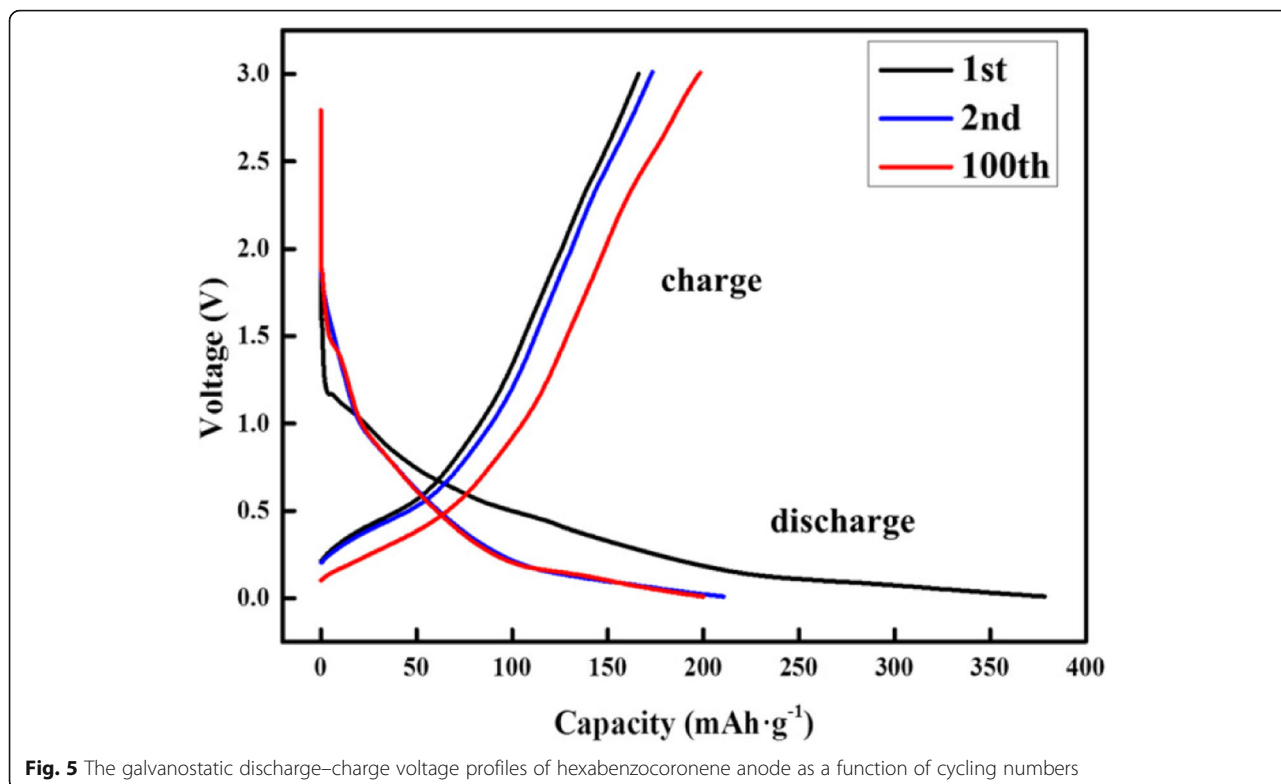
Fig. 5 The galvanostatic discharge–charge voltage profiles of hexabenzocoronene anode as a function of cycling numbers

the hexabenzocoronene. The charging process (Li$^+$ transfer) in hexabenzocoronene anodes requires stabilization. The calculated stabilization HOMO energy of the hexabenzocoronene radical anode ranges from 5.592 V, as shown in Fig. 6b.

The inset in Fig. 7 shows that the assembled multi-structures experienced arranged and rearranged processes. The optimal *d*-spacing between the layers for hexabenzocoronene was examined. This paper revealed a multi-diffusing process of lithium ions as the dynamic structure providing dynamic diffusion paths. TEM showed that lithium diffuses between the layers and has the ability to pass through the sheets, which greatly

increases the lithium ion (yellow spot) diffusion efficiency; the Additional file 1: Figure S1 and Table S1 show adsorption and desorption: V_a/cm^3 (STP) g^{-1} value is 110.47 and 96.62. According to adsorption-desorption isotherm, there is no hysteresis loop in the isotherms of HBC. Moreover, Additional file 1: Figure S2 and Table S2 show BET surface area, and the correlation coefficient value is 0.9999, V_m is 18.647 cm^3 (STP) g^{-1}, and $a_{s,BET}$ is 81.16 m^2 g^{-1}. The TEM image revealed self-assembled structures that were disorganized in the center of the fingerprint, and then they were arranged more regularly into a fingerprint-like structure. In the process of the self-assembly of graphene sheets, graphene sheets

$$HOMO(N0) = 1.770 - 0.508 + 4.33 = 5.592$$
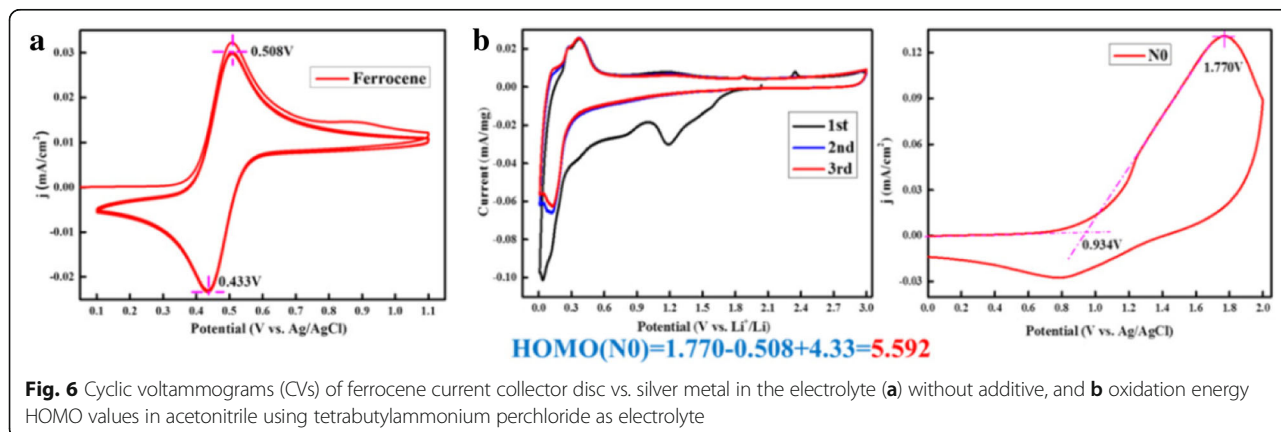
Fig. 6 Cyclic voltammograms (CVs) of ferrocene current collector disc vs. silver metal in the electrolyte (**a**) without additive, and **b** oxidation energy HOMO values in acetonitrile using tetrabutylammonium perchlorate as electrolyte
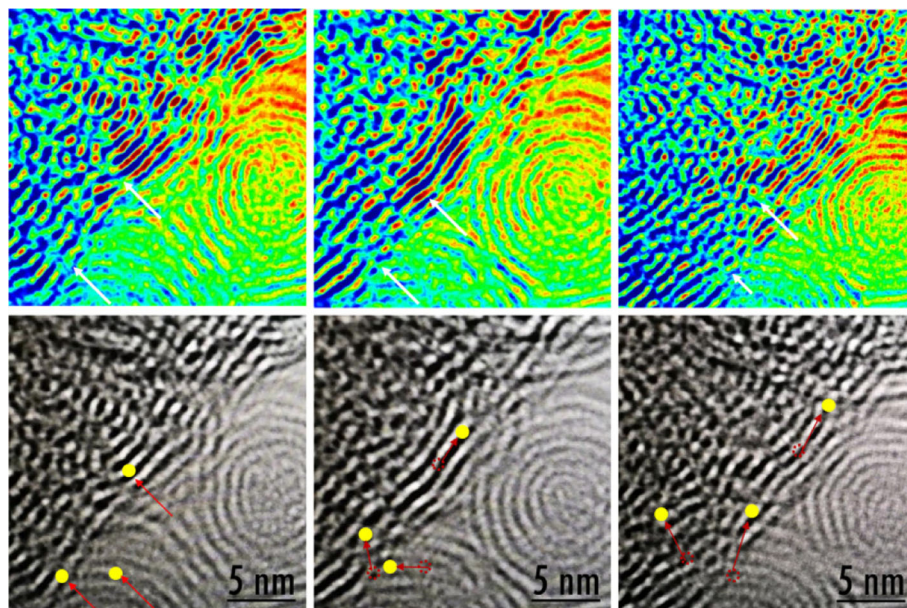
Fig. 7 TEM image of nano-graphene multi-stage self-assembly structure

arrange in a stacked manner and self-assemble into a layered two-dimensional structure in a head-to-head manner. Moreover, the bonding force between molecules is weak with no strong chemical bonds. The self-assembled structure is a dynamic process involving the angular-rearrangement of self-assembled layers of graphene nanosheets under the action of energy. Moreover, TEM image showed that lithium ions have different diffusion modes between the graphene sheets, which can diffuse between the layers and pass through the layers, from the inner layer to the outer layer diffusion. Therefore, nano-graphene exhibits strong lithium ion diffusion properties and surprising lithium ion storage capacity.

Conclusion

HBC shows good structure durability and stability. The electron density with the optimal *d*-spacing in the self-assemblies led to a significantly enhanced LIB anode charge capacity and cycling stability. These results revealed a structure–property correlation between the nature of functional groups and Li storage capacity. Nevertheless, identifying the mechanism for how nano-graphene hierarchically assembles and dominates the overall battery performance will be an important research topic. Through these studies, a more rational and effective application of nano-graphene will be realized. Observing the characteristics of the internal architecture from a microscopic perspective and analyzing the dynamic hierarchical self-assembly properties of a nano-graphene sheet one by one will be the subjects of a future study.

Additional File

Additional file 1: Supporting information (DOCX 436 kb)

Authors' Contributions
Liu R and Jin G designed the experiment and led the project, and Jin G wrote this manuscript. He D and Xiao F performed the SEM and CV calculation measurements. He A performed the TEM and HRTEM measurement. All authors read and approved the final manuscript.

Competing Interests
The authors declare that they have no competing interests

Publisher's Note

Springer Nature remains neutral with regard to jurisdictional claims in published maps and institutional affiliations.

Author details
[1]Affiliated Kunshan Hospital, Jiangsu University, Kunshan 215300, People's Republic of China. [2]College of Vanadium and Titanium, Panzhihua University, Panzhihua 617000, People's Republic of China. [3]School of Pharmacy, Jiangsu University, Zhenjiang 212013, People's Republic of China.

References

1. Halder A, Zhang MW, Chi QJ, Norena LE, Wang JA (2016) Electrocatalytic applications of graphene-metal oxide nanohybrid materials. IntechOpen/books/Adv Cat Mat:379–413
2. Guo SQ, Zhen MM, Liu L, Yuan ZH (2016) Facile preparation and lithium storage properties of TiO2@ graphene composite electrodes with low carbon content. Chem Eur J 22(34):11943–11948
3. Liu H, Shen ZG, Liang SS, Liu L, Yi M, Zhang XJ, Ma SL (2016) One-step in situ preparation of liquid-exfoliated pristine graphene/Si composites: towards practical anodes for commercial lithium-ion batteries. New J Chem 40(8):7053–7060
4. Wang B, Li XL, Zhang XF, Luo B, Zhang YB, Zhi LJ (2013) Contact-engineered and void-involved silicon/carbon nanohybrids as lithium-ion-battery anodes. Adv Mater 25(26):3560–3565
5. Novoselov KS, Geim AK, Morozov SV, Jiang D, Zhang Y, Dubonos SV, Grigorieva IV, Firsov AA (2004) Electric field effect in atomically thin carbon films. Science 306(5696):666–669
6. Novoselov KS, Jiang D, Schedin F, Booth TJ, Khotkevich VV, Morozov SV, Geim AK (2005) Two-dimensional atomic crystals. Proc Natl Acad Sci U S A 102(30):10451–10453
7. Blake P, Brimicombe PD, Nair RR, Booth TJ, Jiang D, Schedin F, Ponomarenko LA, Orozov SM, Gleeson HF, Hill EW (2008) Graphene-based liquid crystal device. Nano Latte 8(6):1704–1708
8. Hernandez Y, Nicolosi V, Lotya M, Blighe FM, Sun ZY, De S, McGovern IT, Holland B, Byrne M, Gun'Ko YK (2008) High-yield production of graphene by liquid-phase exfoliation of graphite. Nature Nanotechnol 3(9):563–568
9. Dreyer DR, Ruoff RS, Bielawski CW (2010) From conception to realization: an historial account of graphene and some perspectives for its future. Angew Chem Int Ed 49(49):9336–9344
10. Li XS, Cai WW, An JH, Kim SY, Nah JH, Yang DX, Piner R, Velamakanni A, Jung IH, Tutuc E (2009) Large-area synthesis of high-quality and uniform graphene films on copper foils. Science 324(5932):1312–1314
11. Bae SK, Kim HK, Lee YB, Xu XF, Park JS, Zheng Y, Balakrishnan J, Lei T, Kim HR, Song YI (2010) Roll-to-roll production of 30-inch graphene films for transparent electrodes. Nature Nanotechnol 5(8):574–578
12. Ohta T, Bostwick A, Seyller T, Horn K, Rotenberg E (2006) Controlling the electronic structure of bilayer graphene. Science 313(5789):313 951–954
13. Virojanadara C, Syvajarvi M, Yakimova R, Johansson LI, Zakharov AA, Balasubramanian T (2008) Homogeneous large-area graphene layer growth on 6H-SiC(0001). Phys Rev B 78(24):245403/1–245403/6
14. Deretzis I, La MA (2016) Simulating structural transitions with kinetic Monte Carlo: the case of epitaxial graphene on SiC. Phy. Rev E 93(3-B):033304/1–033304/9
15. Margulis VA, Muryumin EE, Gaiduk EA (2013) Optical second-harmonic generation from two-dimensional hexagonal crystals with broken space inversion symmetry. J Physics: Condensed Matter 25(19):195302–195313
16. Sevik C (2014) Physical review B: condensed matter. Materials Physics 89(3):035422/1–035422/5
17. Hoang VV, Tai VP, Thinh TK, Giang NH, Qui LN (2017) Ironene—a new 2D material. Comput Mater Sci 126:446–452
18. Singh PK, Sharma K (2018) Mechanical and viscoelastic properties of in situ amine functionalized multiple layer grpahene/epoxy nanocomposites. Curr Nanoscience 14(3):252–262
19. Xu ZG, Tian H, Khanaki A, Zheng RJ, Suja M, Liu JL (2017) Large-area growth of multi-layer hexagonal boron nitride on polished cobalt foils by plasma-assisted molecular beam epitaxy. Sci Rep 7:43100
20. Song L, Liu Z, Reddy ALM, Narayanan NT, Taha-Tijerina J, Peng J, Gao GH, Lou J, Vajtai R, Ajayan PM (2014) Review: Binary and ternary atomic layers built from carbon, boron, and nitrogen. Adv Mater 24(36):4878–4895
21. Velpula G, Li M, Hu Y, Zagranyarski Y, Pisula W, Muellen K, Mali KS, De Feyter S (2018) Hydrogen-bonded donor-acceptor arrays at the solution-graphite interface. Chem Eur J 24(46):12071–12077
22. Park JH, Lee CW, Park JH, Joo SH, Kwak SK, Ahn SN, Kang SJ (2018) Capacitive organic anode based on fluorinated-contorted hexabenzocoronene: applicable to lithium-ion and sodium-ion storage cells. Advan Sci 5(12):1801365
23. Wang X, Zhang C, Xu YF, He Q, Mu P, Chen Y, Zeng JH, Wang F, Jiang JX (2018) A conjugated microporous polytetra(2-Thienyl)ethylene as high performance anode material for lithium- and sodium-ion batteries. Macromol Chem Phys 219(7):1700524
24. He DP, Tang HL, Kou ZK, Pan M, Sun XL, Zhang JJ, Mu SC (2017) Engineered graphene materials: synthesis and applications for polymer electrolyte membrane fuel cells. Advan Mat 29:1–8
25. Mukai K, Harada M, Kikuzawa Y, Mori T, Sugiyama J (2011) Electrochemical properties of hexa-*peri*-hexabenzocoronene in nonaqueous lithium cell. Electrochem Solid-State Lett 14(4):A52–A56
26. Park JH, Lee CW, Joo SH, Park JH, Hwang CH, Song HK, Park YS, Kwak SK, Ahn SH, Kang SJ (2018) Contorted polycyclic aromatic hydrocarbon: promising Li insertion organic anode. J Mater Chem A 6:12589–12597
27. Zhang W, Gu K, Hou PP, Lyu XL, Pan HB, Shen ZH, Fan XH (2018) Hierarchically ordered structures of disk-cube triads containing hexa-peri-hexabenzocoronene and polyhedral oligomeric silsesquioxane. Soft Matter 14(32):6774–6782
28. Dumslaff B, Wagner M, Schollmeyer D, Narita A, Muellen K (2018) A phenylene-bridged cyclohexa-meta-phenylene as hexa-peri-hexabenzocoronene precursor. Chem Eur J 24(46):11908–11910
29. Cui SS, Zhuang GL, Lu DP, Huang Q, Jia HX, Wang Y, Yang SF, Du PW (2018) A three-dimensional capsule-like carbon nanocage as a segment model of capped zigzag [12,0] carbon nanotubes: synthesis, characterization, and complexation with C70. Angewan Chem Inter Edition 57(30):9330–9335
30. Ardhuin T, Guillermet O, Gourdon A, Gauthier S (2018) Molecular resonance imaging and manipulation of hexabenzocoronene on NaCl(001) and KBr(001) on Ag(111). J. Phy. Chem. C 122(22):11905–11910
31. Hassanien AS, Shedeed RA, Allam NK (2016) Graphene quantum sheets with multiband emission: unravelling the molecular origin of graphene quantum dots. J Phy Chem C 120(38):21678–21684
32. Rose P, Emge S, Konig CA, Hilt G (2017) Efficient oxidative coupling of arenes via electrochemical regeneration of 2,3-dichloro-5,6-dicyano-1,4-benzoquinone (DDQ) under mild reaction conditions. Adv Syn Cata 359(8):1359–1372
33. Cao J, Liu YM, Jing XJ, Yin J, Li J, Xu B, Tan YZ, Zheng NF (2015) Well-defined thiolated nanographene as hole-transporting material for efficient and stable Perovskite solar cells. J. A. Chem. Soc. 137(34):10914–10917
34. Liu RL, Wu DQ, Feng XL, Mullen K (2011) Bottom-up fabrication of photoluminescent graphene quantum dots with uniform morphology. J A Chem Soc 133(39):15221–15223
35. Su YL, Yu TW, Chiang WH, Chiu HC, Chang CH, Chiang CS, Hu SH (2017) Hierarchically targeted and penetrated delivery of drugs to tumors by size-changeable graphene quantum dot nanoaircrafts for photolytic therapy. Adv Fun Mate 27:1–12
36. Zhu SJ, Wang L, Li B, Song YB, Zhao XH, Zhang GY, Zhang ST, Lu S, Zhang JH, Wang HY, Sun HB, Yang B (2014) Investigation of photoluminescence mechanism of grapheme quantum dots and evaluation of their assembly into polymer dots. Carbon. 77:462–472
37. Stępień M, Gońka E, Żyła M, Sprutta N (2017) Heterocyclic nanographenes and other polycyclic heteroaromatic compounds: synthetic routes, properties, and applications. Chem Rev 117:3479–3716
38. Walia PK, Pramanik S, Bhalla V, Kumar M (2015) Aggregates of a hetero-oligophenylene derivative as reactors for the generation of palladium nanoparticles: a potential catalyst in the Sonogashira coupling reaction under aerial conditions. Chem Comm 51(97):17253–17256
39. Qin H, Xu T Liu XF (2017) Aerobic oxidation of alkynes to 1,2-diketones by organic photoredox catalysis. Chem Cat Chem 9(8):1409–1412
40. Wang XF, Xu LC, Mu D, Wang H, Feng SY (2016) Silicon effect of dendritic polyphenyl derivatives: enhancement of aggregation-induced emission and emission color adjustment. RSC Adv 6(28):23335–23339
41. Li ZX, Zhang LF, Wang LN, Guo YK, Cai LH, Yu MM, Wei LH (2011) Highly sensitive and selective fluorescent sensor for Zn^{2+}/Cu^{2+} and new approach for sensing Cu^{2+} by central metal displacement. Chem Comm 47(20):5798–5800
42. Tummala NR, Grady BP, Striolo A (2010) Lateral confinement effects on the structural properties of surfactant aggregates: SDS on graphene. Phy Chem ChemPhy 12(40):13137–13143
43. Robinson JT, Zalalutdinov MK, Cress CD, Culbertson JC, Friedman AL, Merrill A, Landi BJ (2017) Graphene strained by defects. ACS Nano 11(5):4745–4752
44. Jayaprakash GK, Casillas N, Astudillo-Sanchez PD, Flores-Moreno R (2016) J Phy Chem A 120(45):9101–9108
45. Huang JR, Lin JY, Chen BH, Tsai MH (2008) Structural and electronic properties of few-layer graphenes from first-principles. Phy Status Solidi B: Basic Solid State Phy 245(1):136–141

46. Ishii J, Matsushima S, Nakamura H, Ikari T, Naitoh M (2016) First-principles calculation study of epitaxial graphene layer on 4H-SiC (0001) surface. J Surface Sci Nanotechnol 14:107–112

47. Huang SQ, Kim KH, Efimkin DK, Lovorn T, Taniguchi T, Watanabe K, MacDonald AH, Tutuc E, LeRoy BJ (2018) Emergence of topologically protected helical states in minimally twisted bilayer graphene. arXiv.org, e-Print Archive. Condens Matter 2018:1–10

48. Han DD, Yan YC, Wei JS, Wang BW, Li TT, Guo G, Yang D, Xie SH, Dong A (2017) Fine-tuning the wall thickness of ordered mesoporous graphene by exploiting ligand exchange of colloidal nanocrystals. Front in Chem 5:1–9

49. Cao J, Zou YX, Gong X, Gou P, Qian J, Qian RJ, An ZH (2018) Double-layer heterostructure of graphene/carbon nanotube films for highly efficient broadband photodetector. Appli Phy Lett 113(6):061112/1–061112/5

50. Wei QL, Wang QQ, Li QD, An QY, Zhao YL, Peng Z, Jiang YL, Tan SS, Yan MY, Mai LQ (2018) Pseudocapacitive layered iron vanadate nanosheets cathode for ultrahigh-rate lithium ion storage. Nano Energy 47:294–300

51. Han JH, Liu P, Ito Y, Guo XW, Hirata A, Fujita T, Chen MW (2018) Bilayered nanoporous graphene/molybdenum oxide for high rate lithium ion batteries. Nano Energy 45:273–279